Karunarathna *et al.*
Geoenvironmental Disasters (2024) 11:8
https://doi.org/10.1186/s40677-024-00270-z

Geoenvironmental Disasters

RESEARCH

Open Access

Identification of the complete particle size distribution of landslide debris by the combined method of scaled image analysis, line-grid analysis and laboratory sieve analysis

Sandaruwan Karunarathna[1,2*], Satoshi Goto[3], Sajith Bandaranayake[1] and Priyantha Bandara[2]

Abstract

Background Ground failures in a slope due to gravity, are commonly known as landslides. Depend on the compositional, geological, and structural characteristics of the unstable initiation zone and the erosional composition of the propagation zone decide the complete particle size distribution of the moving mass and its gradation. This information is most important for the study of downslope movement. Only laboratory sieve analysis cannot fulfil this target because the natural debris contains a wide range of particle sizes, especially boulders. The combined method of scaled image analysis and laboratory sieve analysis or the combined method of line-grid analysis and laboratory sieve analysis was proposed to fulfil the requirement. To study the proposed combined methods, five different locations within the downslope propagation zone from the Aranayake landslide in Sri Lanka were surveyed and analyzed. In image analysis, the high-resolution scaled image of deposited debris was analyzed by computer-based image analysis for particle sizes. Small particles were addressed by the laboratory sieve analysis using the representative debris sample taken from the same location. If the boulder sizes within the debris are too big to address this method, then the Line-grid method was performed. The particles in every 0.5 m along a measured line of debris deposition were measured in this method. If the selected location contains small particles that cannot measured manually, the representative sample was used for the laboratory sieve analysis to fulfil this range.

Results The results of three locations indicated a 40% distribution of < 10 mm and a 60% distribution of > 10 mm representing the general distribution of the debris. Two distributions deviated from the general distribution that was surveyed and analyzed from special locations of the "near boundary of flow path" and "slope change zone" of the landslide.

Conclusions The combined methodology yielded successful results of complete particle size distribution for the wide range of particle sizes in debris. The variation of the particle size distribution curves of debris along the downslope depositions is planned to be used for the study of downslope propagation, damage zone assessment studies, and predicting the representative composition of future failures.

Keywords Scaled image analysis, Line-grid analysis, Particle size distribution curve, Debris, Aranayake landslide

*Correspondence:
Sandaruwan Karunarathna
sandaruwan.nbro@gmail.com
Full list of author information is available at the end of the article

Introduction

A landslide which is also described as mass movement due to gravity is one of the geological processes that lead to the natural shape-up of the geomorphology of the terrain. Landslide is also recognized as a gravitationally driven phenomenon (Hunger et al. 2014) of the product of the denudation process. The landslides occur when the critical combination of internal and external terrain factors (McColl 2022) is met with a triggering event causing a quick increase of shear stress (reduction of shear strength) of the slope material (Nguyen et al 2017). The shear strength (resisting force) of the slope material becomes smaller than the shear stress (driving force) acting on it, resulting in shear failure along a slip surface (Igwe 2014). The material of a "wide range of particle sizes" moves to the downslope due to gravity (Hunger et al. 2014) as a movement type of "flow" defined as debris flow (Varnes 1978). This type of propagation is common in Sri Lanka.

The propagation controlling of failed mass along the downstream depends on the morphology of the downstream (Jeandet et al. 2019), the fluid motion characteristics of the moving mass (Dai et al. 2014; Wu et al. 2022), and the obstacles (Cuomo 2017) which is in the flow path. The deposition of the moving mass mainly depends on the energy loss due to a decrease in the slope angle (Wong and Ho 1996), fluid motion resistance (Takahashi 2007), and obstacles (Cuomo 2017). Though the main deposition generally consists in the low-level altitude zone of propagation, the partial depositions can be also observed just beneath the initiation zone, and flow path/s which depend on the above deposition-controlled criteria. However, the physical composition of the moving mass can be different from place to place. Physical compositions of the moving mass represent the particle size distribution of the debris (Yong et al. 2013), the amount of water, and the other agents that mixed with moveable mass. Generally, other agents such as plant roots, wood particles (Miles 1986), ice particles, construction fragments, etc. differ from one landslide to another. There are no fixed materials for other agents. However, a wide range of particle sizes and water can be generally introduced as physical compositions of the moving mass. The general particle size distribution of debris cannot be measured during its motion. Only can be addressed after the deposition. Thus, the actual water content of debris while its propagation still cannot be addressed. However, the particle size distribution of deposited debris spatially consists of a large amount of information on landslide propagation that is sufficient to study. Thus, the identification of the complete particle size distribution and gradation of landslide debris is highly required to study the downslope propagation characteristics.

The total particle size distribution of deposited debris derived from a failure downstream can vary due to the characteristics of fluid motion (Wu et al. 2022), morphological sorting (Qing-Zhao et al. 2019), and bed and bank erosion (Lyu et al. 2017). Since the grain size variations of the debris in selected locations can be predicted from fine particles to huge boulders, only the laboratory sieve analysis experiment is not vital for this study. Thus, the combined approach of "scaled-image analysis and sieve analysis" or the combined approach of "line-grid method and sieve analysis" were proposed for this study.

Study area

The study focused on the downstream deposition of the Aranayake landslide that started as a slope failure and propagated as a debris flow in Sri Lanka. It was located in the 7.154736 N, 80.430149 E coordinate, based on the WGS84 coordinate system. It occurred 17th of May in 2016 at around 16.30 h. The administrative location of this failure is in Elangapitiya village inside the Aranayake divisional secretariat division within the Kegalle District in Sri Lanka. This failure is known as the most destructive landslide in recent times in Sri Lanka.

The initiation area was recorded as 40,541 m^2 and the total damage area (inside the boundary of the landslide) was identified as 572,953 m^2 (0.57 km^2). The initiation width and length recorded respectively, were 175 m and 243 m. 25 maximum initiation depth was measured in the crown area of this landslide. The initiation zone consisted of partly tea plantation land use and degraded forests in the mountain called "Samsara Kanda". It recorded 31 deaths and 96 missing (bodies were not found) with 53 houses completely damaged and buried. Three main safe zones can be identified within this landslide boundary and one house was fortunately safe inside this safe zone. There were three main flow paths during the propagation. All three flow paths were combined together in the later stage of the downstream and propagated through the main valley.

The study area was selected including the Aranayake landslide and surrounding area (Fig. 1) that can visualize the surface morphology of the terrain (Fig. 2) for the study purpose. The study area was identified as 5.4 km^2 of the area and it contained parts of the seven administrative villages called Elangapitiya, Debathgama Pallebage, Debathgama Udabage, Kalugala, Hathgampala, Ganthuna Udagama, and Narangala (Fig. 1). However, the landslide was only contained within the Elangapitiya and Debathgama Pallebage Villages (Fig. 1). The Aranayake Landslide was started from Elangapitiya village and the main deposition was observed within the Debathgama Pallebage Village (Fig. 1). Though the main deposition was observed in the low-level altitude in Debathgama

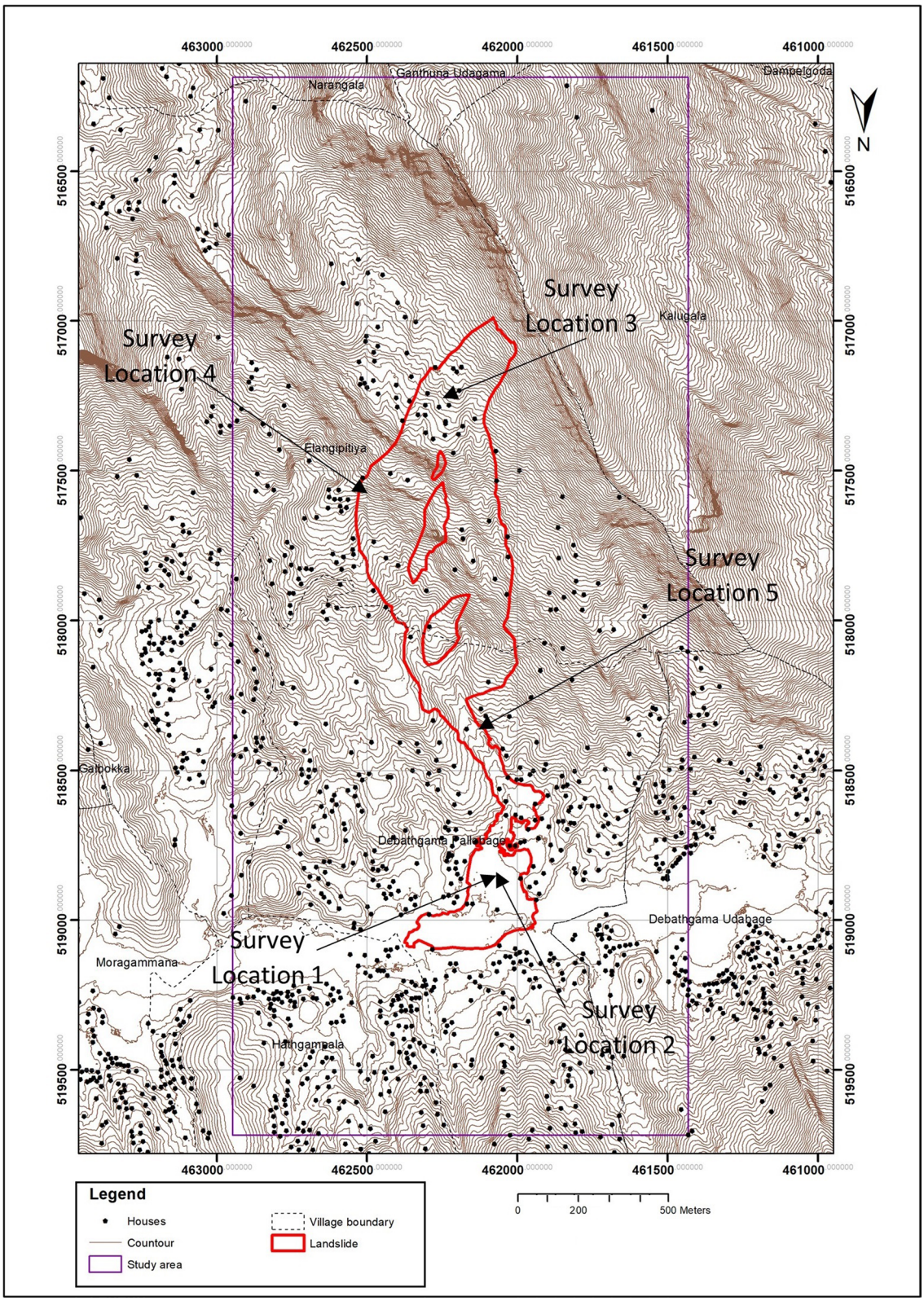

Fig. 1 Focused area of Aranayake landslide

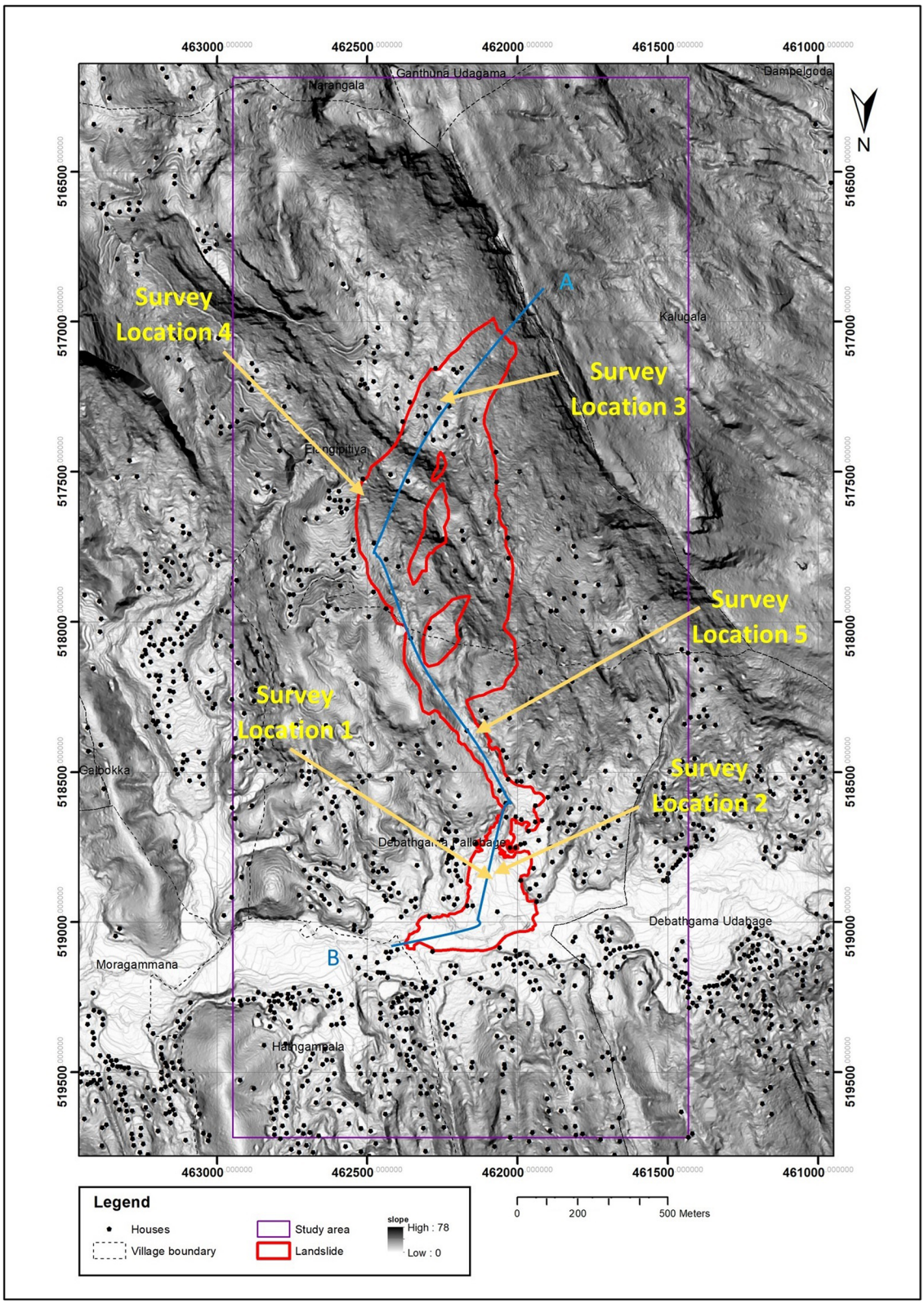

Fig. 2 Morphology of the terrain in study area (before failure)

Pallebage village, there were partial depositions observed just downstream from the initiation zone and within the different locations in flow paths. The survey was focused on the complete particle size distributions of the downstream. Thus, five survey locations were selected within the study area (Fig. 1).

Survey location one and survey location two were selected within the representative locations of the deposition inside the final spreading propagation zone of the debris flow (Fig. 1). The first location was located near the naturally prepared stream and the second location was located the most representative zone for spreading propagation of landslides without disturbing the surface runoff. The third survey location was selected within the partially deposited debris zone in the high-altitude area located just downstream of the initiation zone of the landslide. The fourth location was planned to select one of the flow paths from three flow paths. However, the middle propagation area of the flow path was not representative because of the possibility of changes of the deposited debris with time by erosion from water runoff after landslide due to the valley morphology. Thus, the fourth location was selected within the partial deposition zone of the right-side flow path near the propagation boundary.

The initiation zone where the landslide started was positioned in escarpment slope terrain geologically. From the initiation zone to the middle propagation zone was identified as very steep (Fig. 2). Then the steep slope suddenly changed to gentle further downstream of the propagation occurred (Fig. 3). The fifth location was selected just downstream of the slope change from steep to gentle. Also, the selection of the fifth survey location considered the zone of three flow paths combined together.

Methods

The combined methodology of the scaled-image analysis and the laboratory sieve analysis or the combined methodology of line-grid analysis and laboratory sieve analysis

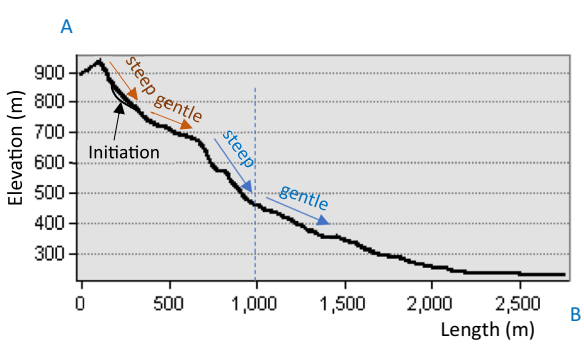

Fig. 3 Profile of the section indicated in Fig. 2

was proposed for the debris that contained a wide range of particle sizes in failure. The idea of the scaled image analysis can be expressed as the particle size distribution identification using the high-resolution images captured with two-sided scales from the surface of a landslide deposition. However, the difficulty of detecting very small particles precisely from the scaled image, this test requires a combination of another test (laboratory sieve analysis test) for the complete particle size distribution. If it's difficult to capture a scaled image of a surface of debris contained with huge boulders, the Line-grid analysis was introduced later. Since the failures in metamorphic terrains generally consist of a wide range of particle sizes, the debris of the Aranayake landslide was highly appropriate to study.

The possible deposition locations were pre-estimated (Fig. 1) by the geomorphological landform of the study area (Fig. 2) prepared using LiDAR data (1 m resolution raster analysis by Arc GIS). The locations that were required to survey in the Aranayake landslide were planned from the estimated zones for debris depositions along the flow path and the main deposition in the low altitude zone. The two locations from the spreading zone were planned to be surveyed in the low altitudes of deposition. One location was currently near the new natural stream and possible to deviate from the actual deposition. The other location within the spreading zone of low altitude was the most representative location due to the low possibility of deviation (by erosion from surface runoff) from the actual condition of deposition. Another location was selected just downstream of the initiation zone of the landslide (high altitude). The next location was selected from the flow path (near the landslide boundary of the right-side flow path out of the three flow paths). The last location was selected from the location of slope changes from steep to gentle with all flow paths combined together.

The vertical cross-section cuts were prepared carefully without disturbing the natural deposition in every selected location. The scaled high-resolution images were perfectly taken from the representative undisturbed cross-sections of the landslide deposition locations in the field survey. The scaled images were taken by three cameras avoiding the topmost layer of the deposition. Deciding the sectional area for the scaled image analysis generally depends on the particle sizes deposited in the survey location. All particle sizes should be representatively covered (inside the selected area) to capture the scaled image for the analysis. This is generally an experience-based decision. An increase in accuracy can be expected if the sector area is increased. However, the analysis time will increase due to the number of particles increases. If the particle size is too large to decide the

sectional area for the scaled image analysis, the proposed Line-grid method should be followed.

To ensure the reliability of the outcomes, the survey method should be carefully handled. Specially selecting the best location for the survey in the field, the minimum disturbance to the deposited location should be carefully selected. The deposited debris should not be disturbed due to the post erosion internally and the deposited particles should not be changed due to plant roots or burrows dug by animals. Special attention is required to select the minimum groundwater percolation location. When capturing the image, the camera angle should be perpendicular to the cut and not too close to the cut to prevent small distortion of the image in corners.

These images were analyzed to identify each particle by the computer-based scaled image analysis software. The diameters of each particle were measured from the computer-based scaled image analysis. Two perpendicular diameters of the debris particle were focused in this method (Fig. 4). Very small particles of the vertical

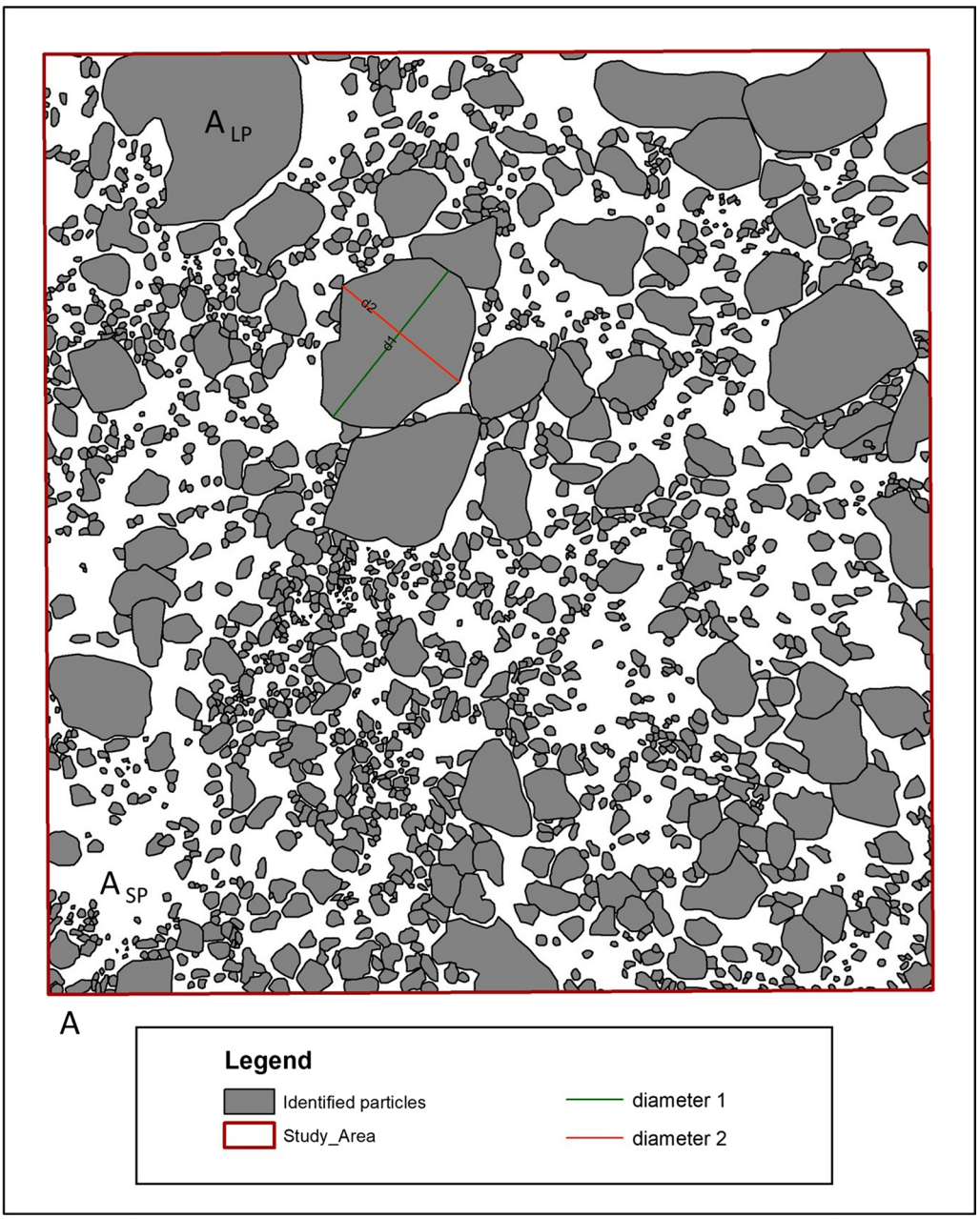

Fig. 4 An example of the scaled image particle size distribution analyses

cross-section were not clearly visible to identify by the scaled image compared to the resolution of the camera. Thus, the particle sizes of small particles that consist in the area that cannot be identified visually by the scaled image in this analysis need to be determined by another method and need to be combined together. Thus, the laboratory sieve analysis was proposed for this gap-filling method. The representative sample for fine particles in scaled image analysis locations needs to be obtained in the exact location where the picture was taken for the laboratory sieve analysis. The particle size distribution curves obtained from scaled image analysis (for large particles that can be visually identified from the scaled image) and sieve analysis (for small particles that cannot be visually identified from the scaled image) should be combined together to visualize the total complete particle size distribution of the debris. The area percentages of the small particles and large particles were used for the combined process.

Figure 4 was used as an example to explain the combining process of the scaled image analysis result and the laboratory sieve analysis results together. In Fig. 4, A_{LP} represents the total area of large particles that can be identified by a scaled image, A_{SP} represents the total area of small particles that cannot be identified by a scaled image, and A represents the total scaled image analysis area. 0.48 (48%) was measured as an answer for the A_{LP}/A from Fig. 4. This percentage was named as "small sediment ratio". Using this percentage value, the large particle distribution should be plotted from 48 to 100% in the y-axis of the particle size distribution curve (Fig. 5). The plot from 0 to 48% will be obtained by the laboratory sieve analysis from the representative sample that obtained from the exact location of this picture was taken.

Two perpendicular diameters of the particles measured from the scaled image analysis were used to calculate the frequencies of their mean diameter values. The cumulative frequencies of the mean diameter values were used to plot the particle size distribution curve from scaled image analysis. The complete particle size distribution curve can be prepared by combining the laboratory sieve analyses data that rearranged from 0 to 48% percentages in the case of the example given in Fig. 4. This method was used for the combining process of the results obtained from the above-analyzing methods together.

The scaled image analysis method can be introduced as a two-dimensional analysis. Three-dimensional characteristics of particle sizes were not identified from this method. Thus, the deviation of the results of two-dimensional analysis compared to three-dimensional analysis needs to be checked through accuracy assessments.

The line-grid method for particle size distribution is generally applicable to new deposits that have no considerable changes from original deposits in the deposition surface. Also, it was very useful for the big-size boulder concentrated zones that were not applicable to the scaled image analysis. The line-grid method analyzed surface deposit particles. Not for the vertical cross-sections. Thus, the old depositions do not give considerable accuracy due to changes in the characteristics of the deposition in time due to surface erosion and weathering. The

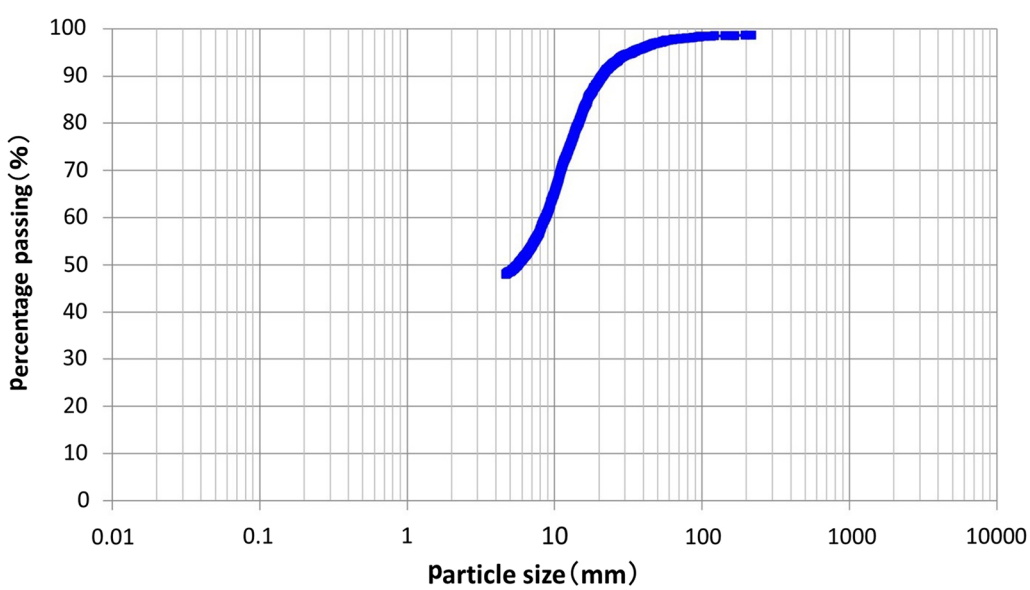

Fig. 5 An example of the particle size distribution analyses of large particles (prepared using Fig. 4)

perpendicular three-diameter values (three-dimensionally surveyed) were recorded for each particle which is deposited every 0.5 m along a measured line of debris deposition (Fig. 6). These data were used to calculate the mean diameter of each particle and their counts. If the location of the 0.5 m interval consists of small particles that are not applicable to measure diameters by a ruler, these locations were recorded as "small particle locations". The count of the "small particle location" compared to the total locations taken from the line-grid method represents the fine sediment ratio of this method.

The small particle size distribution that cannot be measured directly from a field survey was obtained by laboratory sieve analysis using the representative sample obtained from the representative location of the line-grid survey. The cumulative frequencies of the mean diameter values were replaced y-axis of the particle size distribution curve plot. This represented the particle size distribution curve of large particles that were plotted from the percentage of small sediment ratio to 100%. The complete particle size distribution curve was prepared by combining the laboratory sieve analysis data that rearranged from 0% to a small sediment ratio percentage to the plot of the line-grid method (Fig. 7).

For this study, the mean diameters of observed particles were used for the preparation of the particle size distribution curves. From picture-based analysis, the mean diameters of particles were used from two perpendicular diameters in two-dimensional analysis. From the line-grid method, the mean diameters of particles were used from three perpendicular diameters in a three-dimensional analysis.

The representative diameter of the particles in standard laboratory sieve analysis is the middle diameters of particles (Fig. 8). If the cross-section of the minimum diameter and middle diameter fits the sieve opening (squire shape), penetration will occur through the sieve opening (Fig. 8). The size of the sieve opening that equal to the minimum diameter of the particle doesn't penetrate because there is another representative diameter perpendicular to it. However, the size of the sieve opening which is equal to the middle diameter meets with the minimum diameter perpendicular to it, will critically penetrate through the sieve opening. Therefore, the critical diameter for penetration through the sieve opening is the middle diameter of the particle. Thus, the middle diameters were used in laboratory sieve analysis for the particle size distribution curves. The laboratory sieve analysis is the standard experiment for the particle size distribution analysis. Thus, the middle diameter analysis is the standard method to prepare the particle size distribution curves. However, the scaled image analysis method doesn't have a way to measure three diameters three-dimensionally. Because this analysis is the two-dimensional method of diameter measurements. Thus, the middle diameter cannot be observed by scaled image analysis but can get the mean diameter of two diameters. To use the scaled image analysis method for research purposes to obtain the particle size distribution analysis, the mean diameter method should be verified. Thus, the

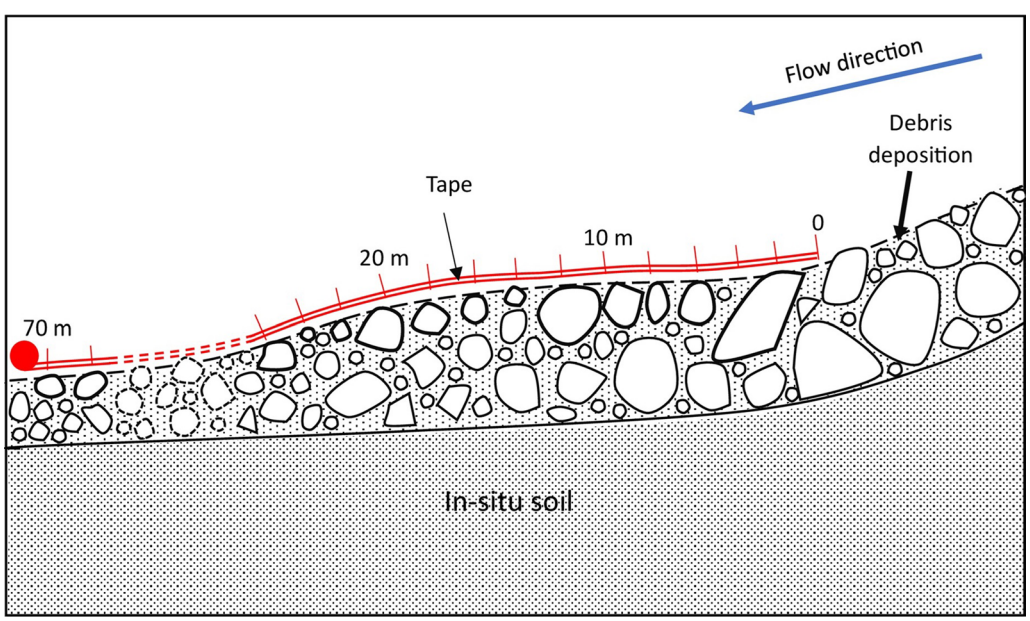

Fig. 6 Line-grid method for the particle size distribution analyses in debris deposition

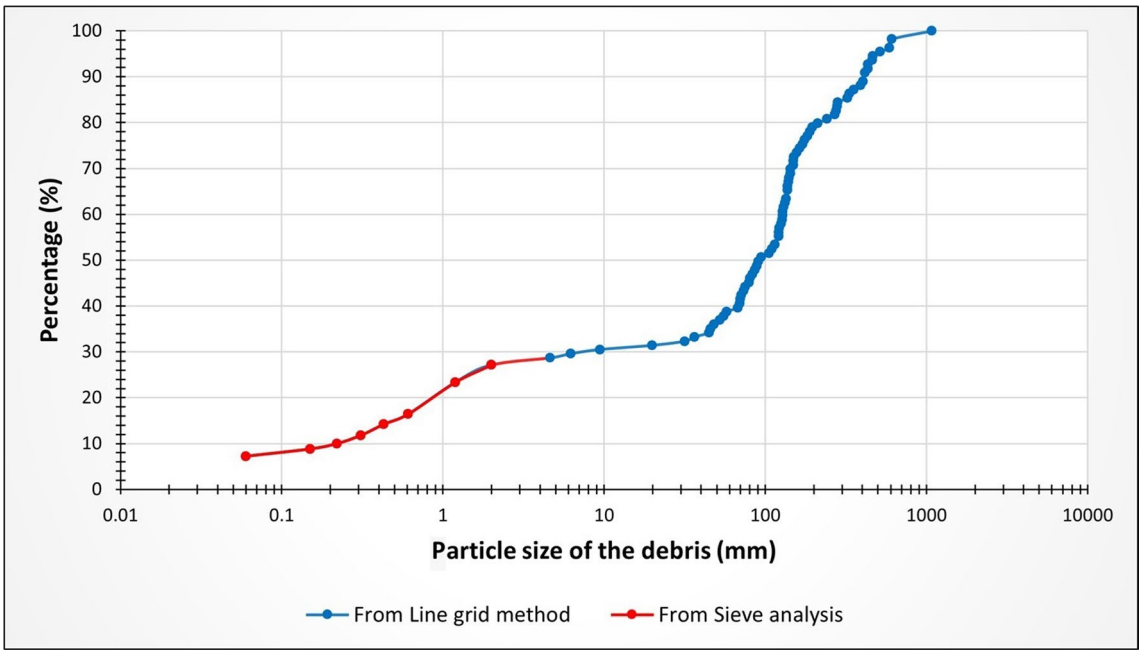

Fig. 7 Particle size distribution of debris in field survey location 5 (small sediment ratio is 27.16%)

mean diameter method needs to be compared with the middle diameter method. If those curves are nearly the same, the scaled image analysis can be verified for the preparation of the particle size distribution curves.

The complete particle size distribution analysis of the cube-shaped sample (20 cm x 20 cm x 20 cm) that was taken from survey location 4 was carried out for this verification purpose (Fig. 9). The obtained full sample was used for the laboratory sieve analysis. The bigger-sized particles that cannot be used for laboratory sieve analysis were collected and manually measured for three perpendicular diameters.

The largest diameter, minimum diameter, and middle diameter were considered while measuring the considerable diameters manually. The middle diameter of all manually measured particles was sorted from smallest to largest with their counts.

Also, the measured diameters of all large particles that were removed from laboratory sieve analysis were used to calculate mean diameters and summarized mean diameters from smallest to largest. The mean diameters and the middle diameters of those particles and their counts were separately used to calculate their frequencies. The frequency of those particles' sizes (mean and middle) was used to calculate the cumulative percentages of the particle size distribution. To obtain the complete particle size distribution of the cube-shaped sample, the laboratory sieve analysis results of the cube-shaped sample were combined using the volume ratio of removed particles from the sieve analysis compared to the total volume in the naturally deposited stage. The comparison of the results of the mean diameter and middle diameter methods leads to verifying the mean diameter methods. When comparing granulometry analysis results from different methods are needed to ensure reliability. Especially when proposing a new method for obtaining the results. Thus, the result obtained by the new method can be compared with the standard accepted method which is generally used scientifically. Thus, the proposed mean diameter method should be verified by comparing it with standard results from middle diameters that are used as particle size distribution analyses. Therefore, the statistical approach was proposed to compare. since the available data bulk exceeds the minimum requirement of the paired T-test, the paired T-test was used for the comparison of two curves. The hypothesis of "there is a significant difference between the two methods" was used. If there is a non-significant small difference between the middle diameter method and the mean diameter method, the proposed mean diameter method can be verified reliably.

Results

The scaled image was analyzed for the identification of particle sizes that can be visually identified by the best pictures taken from the field surveys. Two perpendicular diameters were measured from the identified particles in scaled image analysis (Figs. 10, 11, 12, 13). The priority was given to the maximum diameter of the particle that

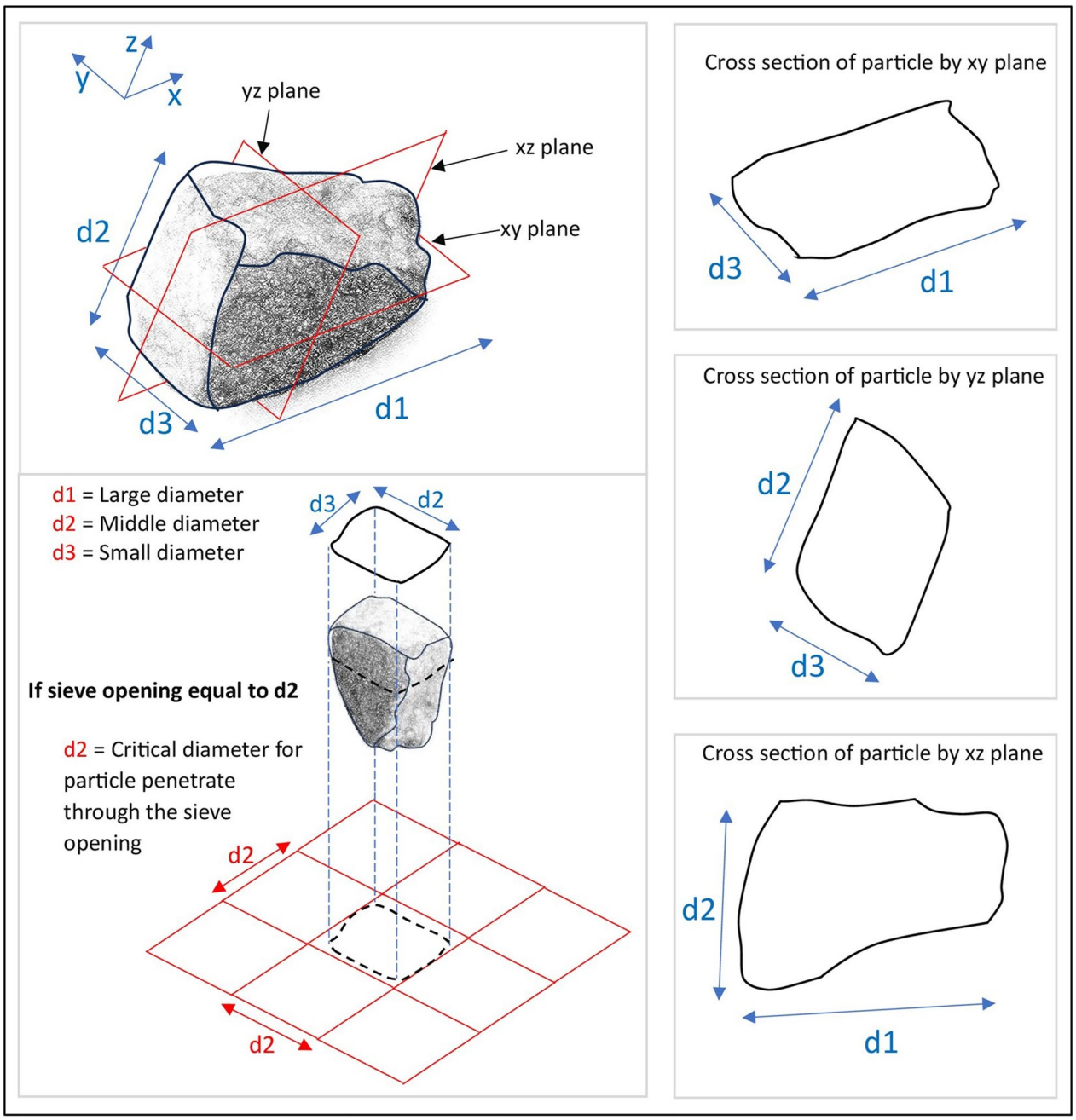

Fig. 8 Middle diameter of a particle effects on the penetration through the sieve opening in laboratory sieves

can be identified by the scaled image and the diameter that is perpendicular to the maximum diameter obtained previously. All possible particles that can be identified visually should be drawn digitally and need to measure diameters (Figs. 10, 11, 12, 13).

The mean values of measured diameters of debris particles were calculated and sorted from the smallest value to the largest value. The frequencies of the mean diameters were calculated with respect to the identified particles. The cumulative frequencies of identified particles were used to plot the particle size distribution curves of the deposited debris considering the small sediment ratio. Small particle distribution was combined for the complete particle size distributions of debris (Fig. 14) using laboratory sieve analysis data rearranged by the small sediment ratio percentage. The logarithmic scale for the

Fig. 9 Cube-shaped sampling from survey location 4

particle sizes obtained by the combined method was used on an x-axis with the units of a millimeter (mm) and the linear scale of the cumulative percentage values of each particle size was used on a y-axis.

The line-grid method is only used in survey location 5. Because the large size boulders were concentrated together due to the energy loss by the sudden change of the general slope angle from 35 to 20 degrees within the path of the debris flow in survey location 5. Also, the main three flow paths were combined together just before the upstream of location 5. The measured three-dimensional data were used to calculate the mean diameters of each particle. The sorted mean diameters and counts were used to calculate the cumulative frequencies for the particle size distribution considering the small sediment ratio. Small particle size distribution was combined to obtain the complete particle size distribution (Fig. 14) using rearranged laboratory sieve analysis data.

The particle size distributions obtained from the combined method of scaled image analysis and the laboratory sieve analysis were plotted together (Fig. 14) and the legends were given as survey location 1, survey location 2, survey location 3, and survey location 4 (Fig. 14). The particle size distributions obtained from the combined method of line-grid analysis and laboratory sieve analysis were potted in the same graph and the legend was mentioned as field location 5 (Fig. 14).

Three particle size distribution curves (Survey locations 1, 2, and 3) obtained from the survey locations in Aranayake failure show considerably the same pattern

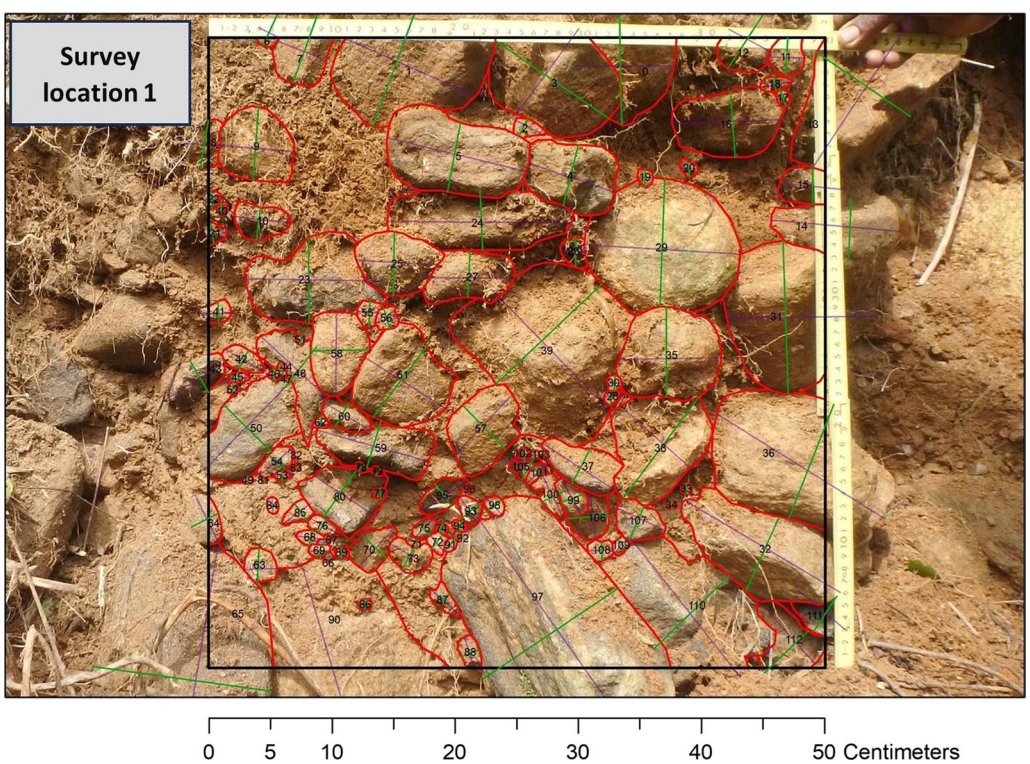

Fig. 10 Scaled image particle size distribution analyses for Location 1 in Aranayake landslide deposit

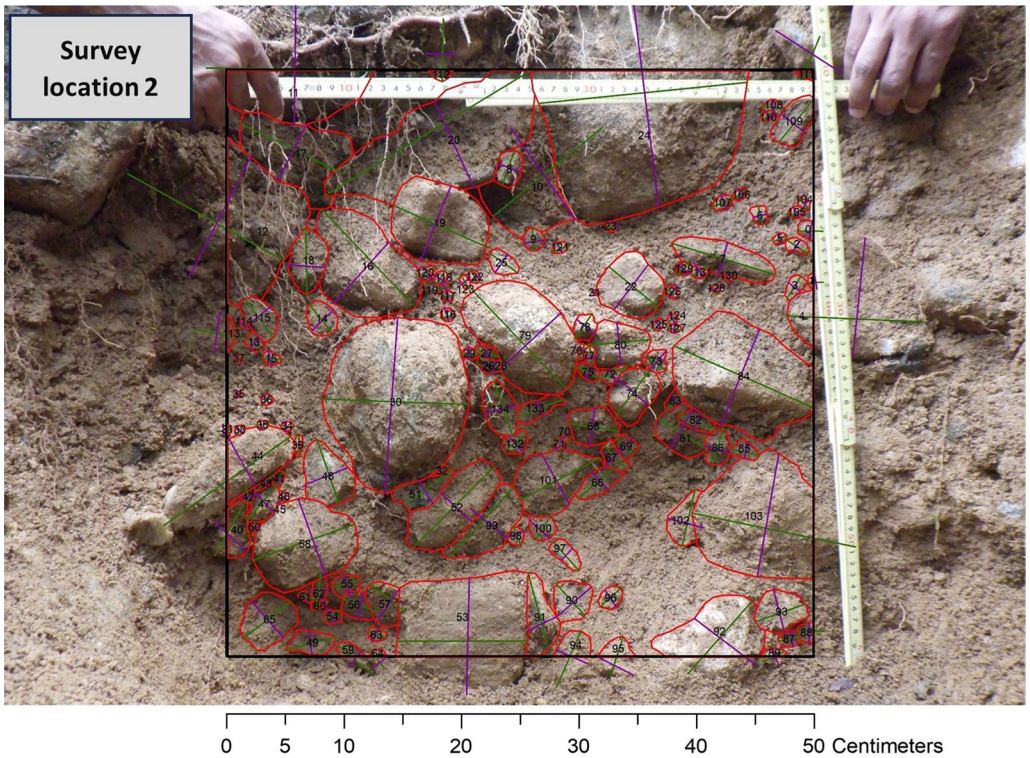

Fig. 11 Scaled image particle size distribution analyses for Location 2 in Aranayake landslide deposit

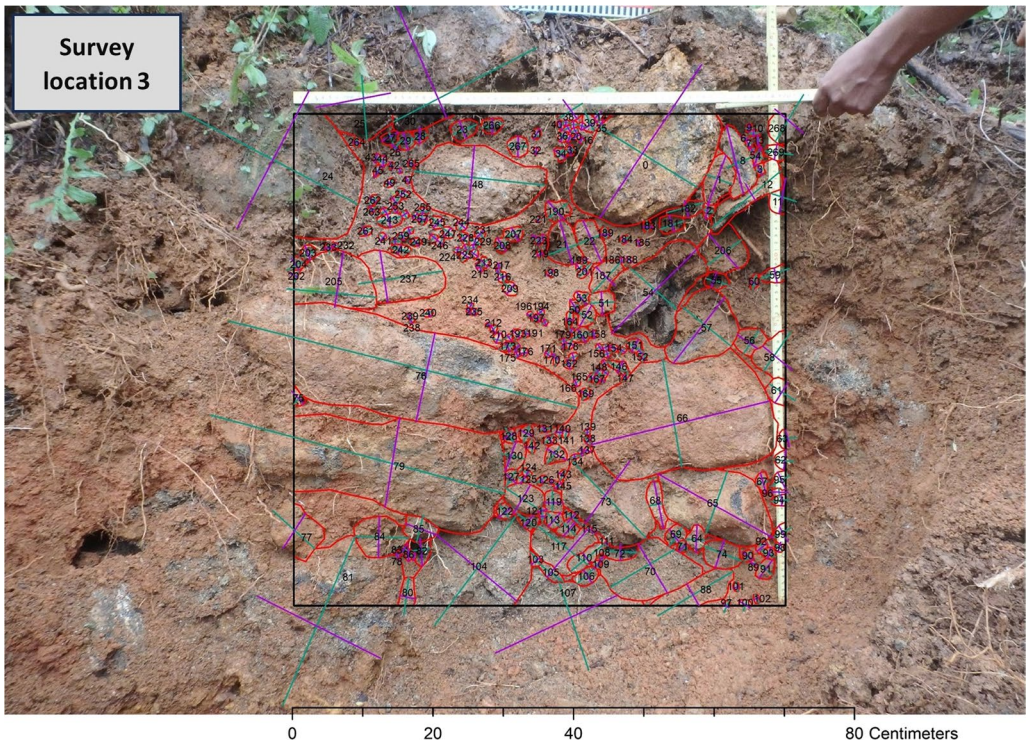

Fig. 12 Scaled image particle size distribution analyses for Location 3 in Aranayake landslide deposit

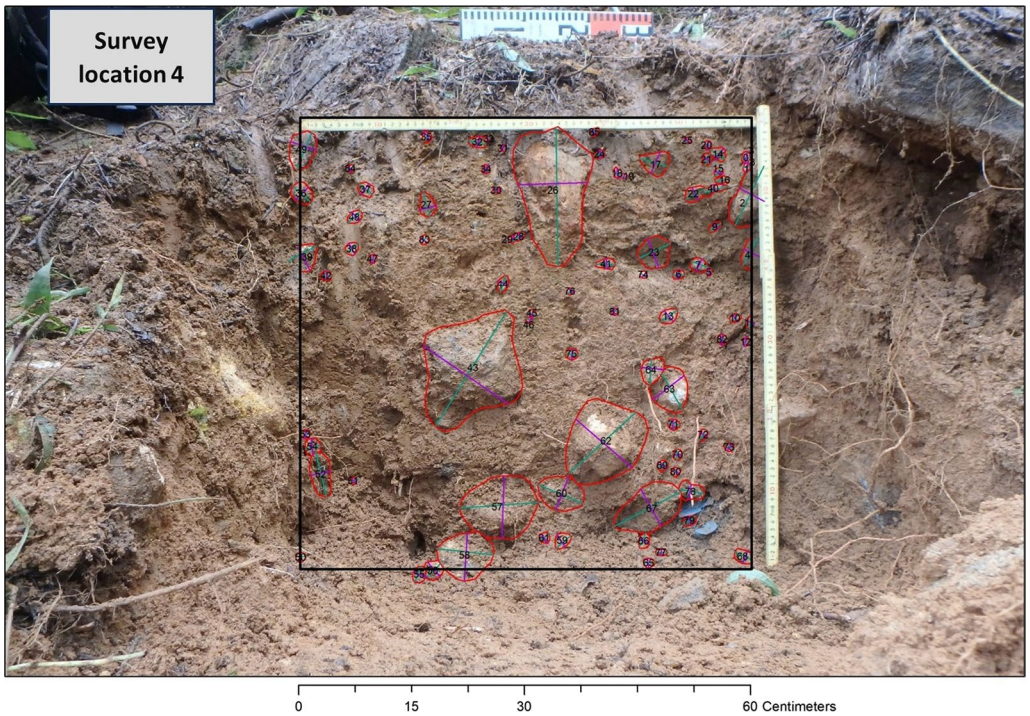

Fig. 13 Scaled image particle size distribution analyses for Location 4 in Aranayake landslide deposit

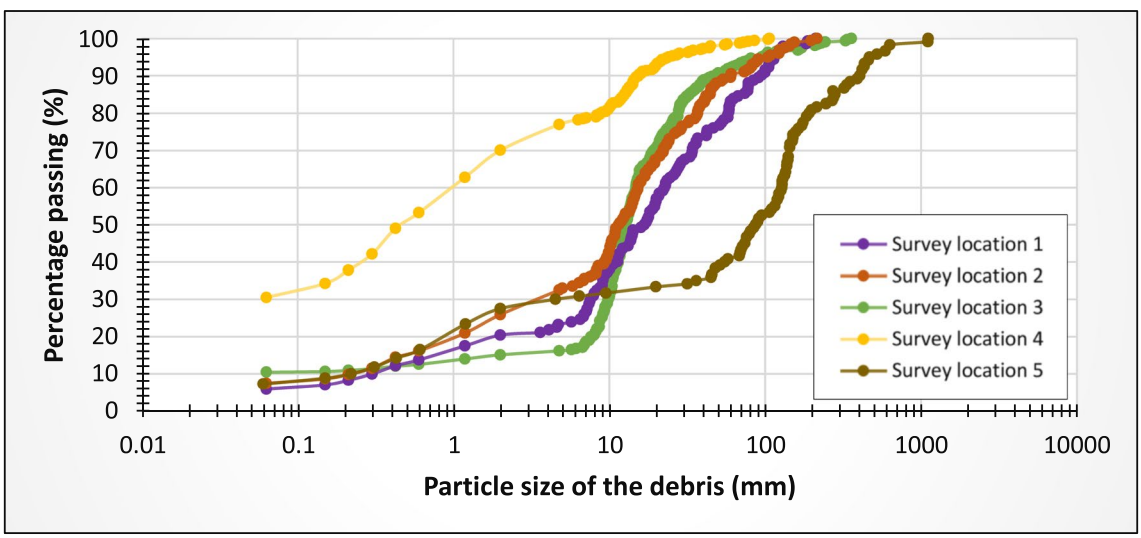

Fig. 14 Particle size distributions of deposited debris in Aranayale failure

(Fig. 14). Other two particle size distribution curves (from Survey locations 4 and 5) are considerably different compared to others (Fig. 14). These two particle size distribution curves (from Survey location 4 and 5) are also different with each other (Fig. 14). Survey location 4 consists of smaller size particle distribution compared to survey location 1,2 and 3. Survey location 4 was selected the deposition occurred near the flow boundary of the flow path which made it possible to sort the particles to the smaller size compared to the general distribution by fluid dynamically. Survey location 5 consists of a large size particle distribution compared to the general particle size distribution due to the morphological sorting. Both deviation of the particle size distribution was further

elaborated in the discussion section. The complete particle size distributions are generally obtained for further study of the landside. Thus, the person who was involved in this study should carefully select the location that related to the objective.

Discussion

Aranayake failure debris contained different sizes of boulders from the bedrock in the initiation zone (Fig. 15) and the steep slope zones in the middle flow path area (Fig. 16). Thus, the total debris distribution curves appeared as continuous two-curve sections (two gaps in gap graded curve) representing both particle size distribution of the moved natural soil combined with large-size boulder distributions (Fig. 14).

The source of the composition of the deposition in location 1 and location 2 can be predicted from both the initiation zone of the landslide and the mass from the erosion throughout the flow paths. Thus, the debris compositions of locations 1 and 2 are the most representative compositions for the study of the propagation of this failure.

However, the particle size distribution of survey locations 1 and 2 indicates a small difference (Fig. 14). The percentage of particles less than 6.5 mm in survey location 1 is a little bit low (about 10%) compared to survey location 2 (Fig. 14). Survey location 1 is currently near to the current natural surface runoff path (stream) in the deposition area. The washing-out of the fine particles to the natural runoff path through groundwater discharge to the stream can be predicted from the debris in location 1. Due to the groundwater discharges, the high chemical weathering of the debris particles can be also predicted compared to survey location 2. Hence, the debris particle distribution percentages of small particles in survey location 1 appeared as low compared to survey location 2 (Fig. 14). Survey location 2 is considerably away (15 m distance to the South-West) from the stream (slope is not to the stream) and can be considered the best location for the debris distribution analysis in the spreading zone.

The sudden change of the slope angle from a steep slope (maximum of 40 degrees) to a gentle slope (minimum of 15 degrees) just downstream of the main initiation area can be observed by the surface morphology analysis (slope shading map in Fig. 2). Therefore, some part of the debris deposited in this zone. Survey location 3 is the target to analyze this distribution that represents the original landslide initiation mass.

The debris particle distribution curve shape in survey location 3 is nearly similar to the particle size distribution of survey locations 1 and 2 (Fig. 14). Thus, the particle size distribution of the landslide initiation is nearly similar to the particle size distribution of final deposition spreading zone (both debris from initiation area and erosions through flow paths). However, the percentage of the fine particles (less than 6.5 mm) of the debris deposited

Fig. 15 Main initiation area of the Aranayake landslide. (Photo source: NBRO database, Sri Lanka; year 2016)

Fig. 16 Middle flow path of the Aranayake Landslide. (Photo source: NBRO database, Sri Lanka; year 2016)

in survey location 3 is low compared to survey locations 1 and 2 (about 10%—20%). However, the percentage of the particle size distribution of > 6.5 mm is high compared to the spreading deposition zone of the landslide. The partially weathered rock fragments that separated apart from the bedrock within the landslide's initiation zone (Fig. 15) were deposited in the zone of survey location 3. However, the huge boulders that gained high kinetic energy were not considerably observed near the surface of the deposited debris in this zone (only a few were observed). Those types of huge boulders can be buried bottom of the debris depositions in this zone or can be moved further downstream with high kinetic energy.

The middle zone of a flow path is naturally converted to surface runoff paths and subsurface runoff paths that can change the original composition of the deposition due to post-erosion and weathering. Representative depositions are not possible in the highest gradient line of the flow paths. Thus, the survey location was focused on the nearest place of the right-side boundary of the right flow path.

The particle size distribution curve of location 4 indicates considerably high fine particle percentages compared to the others. Big-size particles (large mass) of movable debris tend to collect together during motion near the highest gradient flow line (Fig. 17). The low-mass finer particles move towards the low gradient boundaries (Fig. 17). This is the general phenomenon of fluid motions. If depositions occurred in this situation, the flow boundaries contain a finer particle distribution than the depositions in maximum gradient flow lines. However, this distribution is not the representative general composition of the failure. This can be clearly identified by the particle size distributions in survey location 4 compared to the other survey locations (Fig. 14).

Survey location 5 represents the comparatively similar distribution of the particles for less than 10 mm compared with survey locations 1, 2, and 3 (Fig. 14). But results indicated that the curve of survey location 5 (Fig. 14) contains more percentage of large size particles. It looks like large boulders were transported and deposited in this location by the failure compared to the other survey locations. However, the reason for the convergence of the large boulders in one place needs to be clarified. Depending on the morphological analysis, (Fig. 2) survey location 5 is contained inside the zone of the sudden change of slope morphology from a steep slope to a gentle slope. The sudden change of slope from steep to gentle leads to loss of the energy of the large particles and tent to deposit. Also, this zone is just downstream of the confluence of all three flow paths. Thus, all large particles (boulders) flowed through all the flow paths and were deposited in the same zone in which survey location 5 was situated. Therefore, the large-size particle

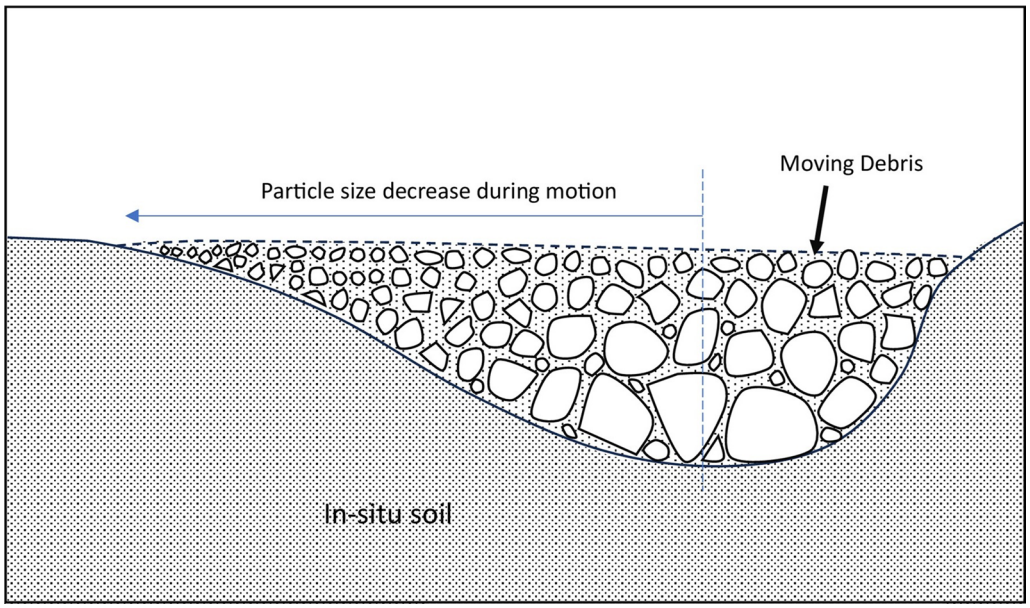

Fig. 17 Debris particles sorting during motion

distributions (boulders) can be clarified in this survey location 5 (Fig. 14).

The cumulative percentages vs particle sizes were plotted (Figs. 18, Fig. 19) to check the comparison of the mean diameter method and middle diameter method. The volume percentage of the large particles that were removed from the laboratory sieve analyses was calculated as 20.65% of the total volume in the natural stage. Thus, the natural volume percentage of the rest particles that were used for the laboratory sieve analysis was calculated as 79.35%. These volume percentages were used to combine the results from laboratory sieve analysis (from 0% to 79.35%) and the manually measured particle frequency percentages (from 79.35% to 100%).

Both the full particle size distribution curve (Fig. 18) and the particle size distribution curve of the removed particles from the laboratory sieve analysis (Fig. 19) indicate nearly similar distributions between the

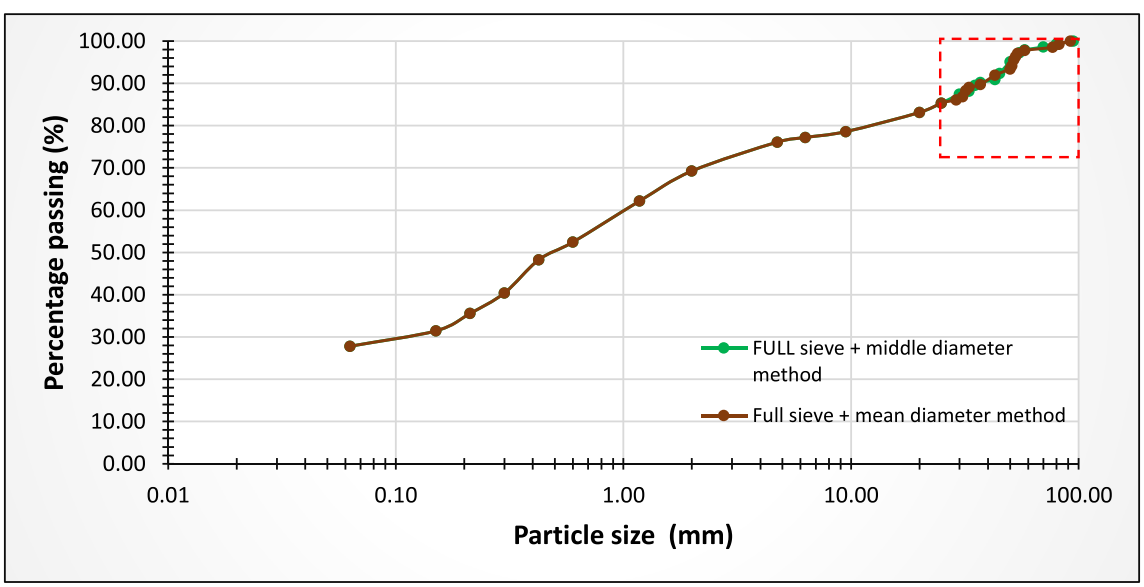

Fig. 18 The complete particle size distribution curves (from middle and mean diameter methods) of the cube-shaped sample obtained from survey location 4

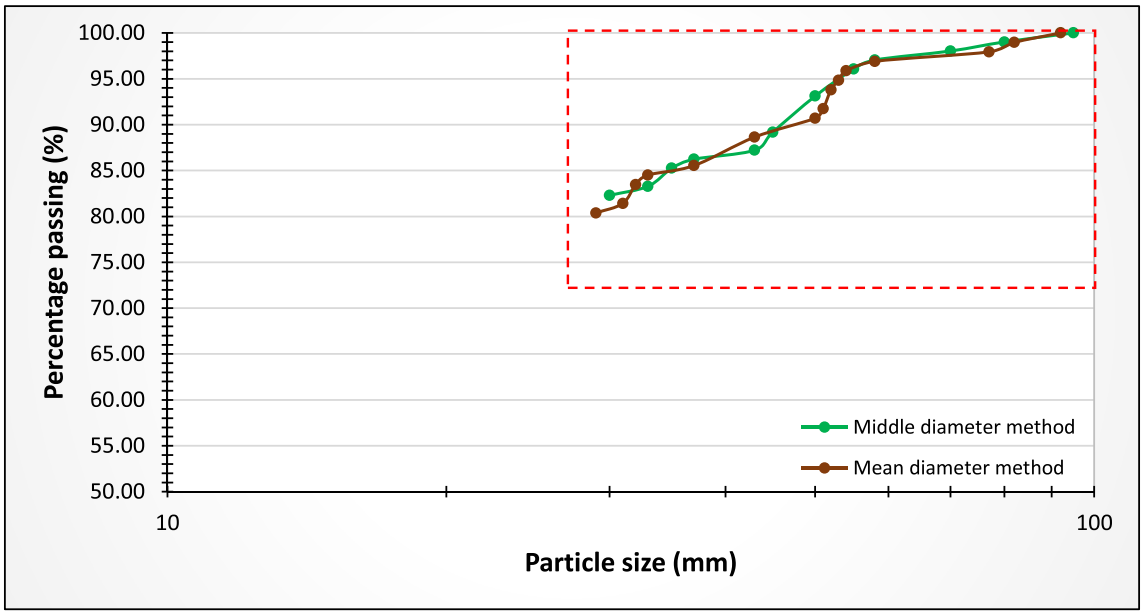

Fig. 19 Particle size distribution curves of the removed particles from the laboratory sieve (the enlargement graph of red dotted area in Fig. 18)

middle diameter and mean diameter method. However, the visual checking of it is not appropriate for the research purpose. Thus, the statistical approach was used to check the similarity of the distribution between the middle diameter method and the mean diameter method.

Since the two results of sieve sizes of each test need to be the same. Therefore, missing data was obtained through linear interpolation (Table 1). The hypothesis of "there is a significant difference between the two methods" was used. The paired t-test was used. The standard deviation of the difference (SD) can be calculated as 0.5302 (Table 1).

$$t = \frac{X - \mu}{SD/\sqrt{n}} \tag{1}$$

where the X is the mean of difference which can be calculated as −5.6225/n = −0.16073 for 35 data. μ is the difference between each mean value.

$$\mu_2 = \frac{2840.233}{35} = 81.15 \tag{2}$$

$$\mu_1 = \frac{2834.608}{35} = 81 \tag{3}$$

$$\mu = \mu_1 - \mu_2 = -0.15 \tag{4}$$

Thus, the t-value and p-value can be calculated as,

$$t = \frac{-0.16073 + 0.15}{0.530/\sqrt{35}} = -0.12 \tag{5}$$

$$\mathrm{p} = 0.9052 \tag{6}$$

Results of the paired t-test indicated that there is a non-significant small difference between the middle diameter method and the mean diameter method (t = −0.12, p = 0.9052, significance level 0.05). Thus, the mean diameter method of the particle size distribution curve can be verified compared with the middle diameter method that is used inside the standard laboratory sieve analysis methods. That indicates the use of mean diameters in the scaled image analysis method and also the line-grid method can be successfully used for the particle size distributions.

Thus, the combined method of laboratory sieve analysis and the scaled image analysis can be verified and also can be indicated as a better method to obtain the particle size distribution analysis for debris with a wide range of particle sizes.

The scaled image analysis of a small area (< 50 cm × 50 cm) may not give better accuracy for the particle size distribution analysis. From the experience, the area should be larger than 50 cm × 50 cm for better accuracy of the scaled image analysis.

Unlike the particle size distribution of natural soils, the graph showing the particle size distribution of debris was

Table 1 Statistical calculation for checking the similarity of curves

Middle diameter method		Mean diameter method		% Difference
Diameter (mm)	%	Diameter (mm)	%	
0.06	27.82	0.06	27.82	0.00
0.15	31.45	0.15	31.45	0.00
0.21	35.58	0.21	35.58	0.00
0.30	40.41	0.30	40.41	0.00
0.43	48.28	0.43	48.28	0.00
0.60	52.45	0.60	52.45	0.00
1.18	62.20	1.18	62.20	0.00
2.00	69.26	2.00	69.26	0.00
4.75	76.11	4.75	76.11	0.00
6.30	77.20	6.30	77.20	0.00
9.50	78.59	9.50	78.59	0.00
20.00	83.13	20.00	83.13	0.00
25.00	85.35	25.00	85.35	0.00
29.00	86.09	29.00	87.03	0.94
30.00	86.46	30.00	87.45	1.00
31.00	86.82	31.00	87.68	0.86
32.00	88.28	32.00	87.91	-0.37
33.00	89.02	33.00	88.14	-0.88
35.00	89.39	35.00	89.54	0.16
37.00	89.75	37.00	90.24	0.49
43.00	91.94	43.00	90.93	-1.01
45.00	92.36	45.00	92.33	-0.03
50.00	93.41	50.00	95.12	1.71
51.00	94.14	51.00	95.54	1.40
52.00	95.61	52.00	95.96	0.35
53.00	96.34	53.00	96.37	0.03
54.00	97.07	54.00	96.79	-0.28
55.00	97.25	55.00	97.21	-0.04
58.00	97.80	58.00	97.91	0.11
70.00	98.27	70.00	98.61	0.34
77.00	98.54	77.00	99.09	0.55
80.00	98.98	80.00	99.30	0.32
82.00	99.27	82.00	99.39	0.12
92.00	100.00	92.00	99.86	-0.14
95.00	100.00	95.00	100.00	0.00
	Sum = 2834.608		Sum = 2840.233	Sum = 5.6225

shown as continuous two-curve sections. It represents the mixing of two types of particles originating from different mechanisms inside the debris. (1) Natural soil originated by in-situ weathering process and (2) the rock fragments of large boulder sizes breaking away from the parent rocks while the failure initiate can be indicated as those two mechanisms.

Identification of the complete particle size distribution of landslide debris is the objective of this study. It is highly required in the downslope propagation studies that are valuable to the potential damage zone prediction for disaster management of a country.

The downslope propagation of a failure depends on the morphology of the downstream (Jeandet et al. 2019), the fluid motion characteristics of the moving mass (Dai et al. 2014; Wu et al. 2022), and the obstacles (Cuomo 2017) that are in the flow path. The surface morphology and the obstacles can be identified by the LIDAR survey of a terrain. Special attention is needed towards the fluid motion characteristics of the moving mass that is controlled by

complete particle size distribution and the water content. Thus, the identification of the complete particle size distribution of debris is highly required to identify how the debris behaves in the propagation stage and stopping stage. Conventionally used laboratory sieve analysis tests do not obtain the distribution of larger particles (especially boulders) within the landslide debris and therefore cannot obtain the total distribution. However, the total distribution of debris controls the downslope propagation. Therefore, the goal is to identify the complete particle size distribution of debris which was studied by this research using different locations of Aranayake failure in Sri Lanka.

As the explanation given above, the complete particle size distribution of five locations indicated that there are large particle size contents that cannot be addressed by only using the conventional laboratory sieve analysis. The proposed two methods successfully addressed the objectives of the research.

The proposed methodologies were not the standard method and also those have a certain degree of innovation. However, the proposed method was compared with the standard method to verify its accuracy in the result.

Conclusions

The combined method of the scaled image analysis and the sieve analysis with the combined method of line grid analysis and the sieve analysis was successfully applied to identify the particle size distribution of debris that contained the vast range of particle sizes downstream of the Aranayake landslide in Sri Lanka. The mean diameter method was used for this analysis and it was verified by comparing it with the middle diameter method's result that is generally used inside the standard laboratory sieve analysis methods.

The study of the deposition in Aranayake failure was carried out in 2022 which is six years after the incident. The plant roots, drifted-wood particles, and other agents that can be decomposed quickly cannot be expected within the debris. The water amount (water content) of the debris also deviated from the actual situation of the propagating stage. Thus, the particle size distribution of the deposition of debris was mainly focused on this study.

The particle size distribution curve obtained from scaled image analysis for a small area can deviate from the actual distribution. Thus, the recommended area should be greater than the area of 50 cm × 50 cm. The selected area for the scaled image analysis from the vertical cut should avoid the topmost layer. Because the composition of the surface can be changed due to erosion by surface runoff and the roots from newly-growth vegetation. The careful cut should be maintained while the cut is prepared without disturbing the deposited particles. Otherwise, the results can deviate from the actual condition.

Even if the particle size distribution is tested without boulder concentrations of debris in general tests, an overview of the whole complete particle size distribution is definitely required to investigate an accurate mechanism of downslope movement of debris. Thus, this study is very important for the research related to the downslope propagation mechanism and damage zone assessment analysis. Especially to the ongoing study of "Potential damage zone prediction of Landslides in Sri Lanka, using the combined approach of Cellular Automaton and Multi-Agent models" (Karunarathna and Goto 2023). The susceptibility zones for landslide initiations are planned to be obtained using the raster slope shading method (Karunarathna et al 2024) to check their potential damage zones. For this Potential damage zone prediction (ongoing) research, the next requirement is obtaining the complete particle size distributions of the debris of pilot sites for the method development. The agent fraction of debris and the particle size distribution are the most sensitive parameters of this ongoing research model. Obtaining the particle size distribution of debris with a wide range of particle sizes, especially with large boulders, is a challenge. The research study introduced in this paper was carried out to develop a better method to obtain the particle size distribution of debris with a wide range of particle sizes and also to obtain the input data for the ongoing research study.

The particle size distribution curve of survey location 2 indicated in Fig. 14 is selected as the most representative physical composition of the debris for Aranayake failure. This result (particle size distribution of the debris in survey location 2) is planned to be used for the ongoing downslope propagation research studies.

Acknowledgements

We thank the Landslide Research and Risk Management Division (LRRMD) of the National Building Research Organization (NBRO) in Sri Lanka for providing the LiDAR data, photos, and required information about the Aranayake failure, and especially for providing the transport facility and other necessary arrangements for the field surveys in Aranayake. Also, we thank the Geotechnical Engineering Division (GED) of the National Building Research Organization (NBRO) in Sri Lanka for providing technical support in field surveys and laboratory test results for the research study. Also, we like to thank Prof. Masataka Shiga, assistant professor, at the Nagaoka University of Technology, and Mr. Dhanushka Jayathilaka, Scientist, National Building Research Organization, Sri Lanka for their kind support in the field survey. The first author is indebted to the Engineering Department, Integrated Graduate School of Medicine, Engineering, and Agricultural Sciences, University of Yamanashi, Japan for providing the working facilities and laboratories for the research work. We also thank the International Consortium of Landslides (ICL), Japan for the technical support for the field survey in Sri Lanka. Same time we also like to thank Prof. Kyoji Sassa, Secretariat in the International Consortium of Landslides (ICL), and Prof. Kazuo Konagai, professor emeritus, at the University of Tokyo for their kind guidance for this research. We also thank the Science and Technology Research Partnership for Sustainable Development (SATREPS) for the funding support for the research.

Author contributions
All authors including the first author gave their onsite contribution to the field survey. The corresponding author analyzed the data and wrote the manuscript. SB gave his contribution to the statistical analysis to check whether the result graphs from the two methods were nearly the same or not. SG supervised the whole steps of this research. All authors checked and approved the final manuscript of this research.

Funding
The research is funded by the Science and Technology Research Partnership for Sustainable Development (SATREPS), Japan.

Availability of data and materials
The data that was used for the findings of this study are available in the database of the National Building Research Organization and also shared with the Engineering Department, Integrated Graduate School of Medicine, Engineering, and Agricultural Sciences, University of Yamanashi, Japan.

Declarations

Competing interests
The authors declare that they have no competing interests.

Author details
[1]Faculty of Engineering, Integrated Graduate School of Medicine, Engineering, and Agricultural Sciences, University of Yamanashi, Kofu, Japan. [2]Landside Hazard Mapping Project, Landslide Research and Risk Management Division, National Building Research Organization, Colombo, Sri Lanka. [3]Faculty of Engineering, Graduate Faculty of Interdisciplinary Research, University of Yamanashi, Kofu, Japan.

Received: 13 December 2023 Accepted: 1 February 2024
Published online: 15 February 2024

References
Cuomo S, Cascini L, Pastor M, Petrosino S (2017) Modelling the propagation of debris avalanches in presence of obstacles. In: Advancing culture of living with landslides: Volume 3 advances in landslide technology, Springer International Publishing, pp 469–475
Dai Z, Huang Y, Cheng H, Xu Q (2014) 3D numerical modeling using smoothed particle hydrodynamics of flow-like landslide propagation triggered by the 2008 Wenchuan earthquake. Eng Geol 180:21–33
Hungr O, Leroueil S, Picarelli L (2014) The Varnes classification of landslide types, an update. Landslides 11:167–194
Igwe, (2014) The analysis of rainfall-induced slope failures at Iva Valley area of Enugu State Nigeria. Environ Earth Sci 71:2465–2480
Jeandet L, Steer P, Lague D, Davy P (2019) Coulomb mechanics and relief constraints explain landslide size distribution. Geophys Res Lett 46(8):4258–4266
Karunarathna S, Goto S (2023) Potential damage zone prediction of rain-induced rapid and long traveling landslides in Sri Lanka, based upon debris flow analysis combining cellular automation and multi-agent models [conference presentation abstract]. Session 1.1-International program on landslides and global and international activities for KLC2020 (part II), 6th World Landslide Forum, Florance, Italy. https://webapp.oicgroup.it/wlf6/abstract/15/1.1-19.pdf.
Karunarathna S, Bandara P, Goto S, Bandaranayake S (2024) Identification of potential natural slope failure zones by geomorphological analyses using raster slope shading of LiDAR; case study from Kegalle, Sri Lanka. Progress in Landslide Research and Technology - volume 3 issue 1, to be published (accepted)
Lyu L, Wang Z, Cui P, Xu M (2017) The role of bank erosion on the initiation and motion of gully debris flows. Geomorphology 285:137–151
McColl ST (2022). Landslide causes and triggers. In: Landslide hazards, risks, and disasters, Elsevier, pp 13–41
Miles DWR, Swanson FJ (1986) Vegetation composition on recent landslides in the Cascade Mountains of western Oregon. Can J for Res 16(4):739–744
Nguyen TS, Likitlersuang S, Ohtsu H, Kitaoka T (2017) Influence of the spatial variability of shear strength parameters on rainfall induced landslides: a case study of sandstone slope in Japan. Arab J Geosci 10(16):369
Qing-Zhao Z, Qing P, Ying C, Ze-Jun L, Zhen-Ming S, Yuan-Yuan Z (2019) Characteristics of landslide-debris flow accumulation in mountainous areas. Heliyon 5(9)
Takahashi T (2007) Progress in debris flow modeling. Progress in landslide science, 59–77
Varnes DJ (1978) Slope movement types and processes. Spec Rep 176:11–33
Wong HN, Ho KKS (1996) Travel distance of landslide debris. In: Proceedings of the 7th international symposium on landslides, Trondheim, Norway, Vol 1, pp 417–422
Wu Y, Shao K, Piccialli F, Mei G (2022) Numerical modeling of the propagation process of landslide surge using physics-informed deep learning. Adv Model Simul Eng Sci 9(1):1–15
Yong L, Xiaojun Z, Pengcheng S, Yingde K, Jingjing L (2013) A scaling distribution for grain composition of debris flow. Geomorphology 192:30–42

Publisher's Note